Viscoelastic Characterization of Polymers Using Instrumented Indentation. II. Dynamic Testing

C. C. WHITE,[1] M. R. VANLANDINGHAM,[1*] P. L. DRZAL,[1] N.-K. CHANG,[2] S.-H. CHANG[2]

[1]National Institute of Standards and Technology, Gaithersburg, Maryland 20899-8615

[2]Department of Mechanical Engineering, National Taiwan University, Taipei, Taiwan

Received 4 October 2004; revised 12 January 2005; accepted 20 February 2005
DOI: 10.1002/polb.20455
Published online in Wiley InterScience (www.interscience.wiley.com).

ABSTRACT: Dynamic nanoindentation was performed on a cured epoxy, a poly(methyl methacrylate) (PMMA), and two poly(dimethyl siloxane) (PDMS) samples of different crosslink densities. These samples were used to compare dynamic nanoindentation with classical rheological measurements on polymeric samples in the glassy and rubbery plateau regions. Excellent agreement between bulk rheological data and dynamic nanoindentation data was observed for the two glassy materials (epoxy and PMMA) and the less compliant PDMS sample. More divergent results were observed for the more compliant PDMS sample. The theoretical foundation and historical development of the working equations for these two types of instrumentation are presented and discussed. The major difference between nanoindentation and the more classical rheological results is in the treatment of the instrument–sample interface.
 J Polym Sci Part B: Polym Phys 43: 1812–1824, 2005
Keywords: mechanical properties; nanotechnology; rheology

INTRODUCTION

Recent commercial development of instrumented indentation or nanoindentation systems has resulted in improvements in quasi-static force sensitivity[1] and the advent of dynamic testing with harmonic force–displacement capabilities.[2] These developments have generated scientific interest in the use of these instruments to characterize the mechanical response of soft materials such as plastics, rubbers, gels, and biological materials. Potential benefits of using nanoindentation to characterize soft materials include (1) the ability to probe the mechanical response with submicrometer spatial resolution both laterally across the surface and through the thickness and (2) the ability to measure time-dependent properties with relatively small amounts of material. However, soft materials can contemporaneously store and dissipate applied mechanical energy, and so the transformation between the measured instrumental response and actual sample properties obtained from an indentation measurement is more difficult to interpret than that for more traditional engineering materials, such as metals or ceramics. Thus, these materials present a major challenge to the application of this technology.

The application of electromagnetic and electrostatic transducers to instrumented indenta-

Certain commercial instruments and materials are identified in this article to adequately describe the experimental procedure. In no case does such identification imply recommendation or endorsement by the National Institute of Standards and Technology or U.S. Army Research Laboratory, nor does it imply that the instruments or materials are necessarily the best available for the purpose.

**Present address:* U. S. Army Research Laboratory, Aberdeen Proving Ground, Maryland 21005

Correspondence to: C. C. White (E-mail: christopher.white@nist.gov)

Journal of Polymer Science: Part B: Polymer Physics, Vol. 43, 1812–1824 (2005)

tion systems has brought about substantial improvements in the control and detection of forces and displacements at very low levels, resulting in tip–sample contact dimensions as low as hundreds of nanometers. Additionally, these control and detection systems are virtually identical to those used in commercial rheometer instrumentation. To enhance the low force capabilities of instrumented indentation systems, dynamic capabilities have been developed, in which small-amplitude (1 nm) harmonic oscillations are superposed over a quasi-static loading history. The development of a dynamic modulation method, sometimes called the continuous stiffness method (CSM), was based on a dynamic model of the instrument and the assumption of zero energy loss at the tip–sample interface. This method allows indentation modulus and hardness values to be calculated throughout the loading history, as opposed to a single set of values calculated from the unloading data with more traditional indentation analysis. Additionally, measures of the dynamic performance of the instrument provide a means for sensitive detection of the initial point of tip–sample contact, which can be a large source of uncertainty in indentation measurements of soft materials. Recently, the CSM method has been used to measure the dynamic response of the sample over a range of frequencies, including calculations of the energy storage and loss, similarly to more classical rheological measurements. In this case, instead of the assumption of no damping at the tip–sample interface, the stiffness of the load frame is taken to be infinite.

The ability to characterize the viscoelastic response of small volumes of material is an important for using nanoindentation to characterize soft materials. Commercial rheometers require gram quantities of a sample and determine mechanical properties averaged over the entire sample. Often, research-grade materials cannot be initially produced in sufficient quantities for such measurements. Combinatorial approaches to material development also require measurement capabilities that can be applied to small amounts of material. Although many isotropic, homogeneous samples are accurately approximated by average properties, location-specific or surface-sensitive measurements are often required for characterizing many soft materials of interest, such as thin polymer films, polymer blends, copolymers, polymer composites and other filled systems, and biomaterials. However, fundamental differences exist between rheometry and nanoindentation systems that arise from the divergent historical development of these instruments. Exploring this history, including the relevant physics and analyses, may provide a framework for bridging these measurement techniques.

HISTORICAL COMPARISON OF INDENTATION AND RHEOLOGY

Instrumented indentation is a well-developed experimental technique for measuring the properties of hard materials, such as minerals, ceramics, and metals. The overall constitutive behavior for these traditional engineering materials generally conforms to elastic–plastic models, including a single real stiffness parameter and little-to-no sensitivity to the difference between compressive and shear strain. Elastic–plastic constitutive models have been used to describe the indenter–sample interaction with a single characteristic strain level, even though the contact geometry produces a large range of strain levels.[3] Additionally, for the elastic–plastic model, the dominant mechanism of energy transfer at low strain levels and short time frames is elastic (i.e., energy storage), whereas for higher strains and longer time frames, the mechanism is plastic (i.e., energy dissipation). Because the sample may be rigid, the compliance of the instrument can often be a significant fraction of the total response and thus must be calibrated.

In contrast, classical rheology focuses on the response of soft materials or liquids to very small time-dependent applied strains. The measured response of these soft materials often involves simultaneous energy storage and energy dissipation, and the two mechanisms can be roughly equal in magnitude.[4] Describing the resulting time-dependent stress of soft materials subjected to small applied strains often requires a viscoelastic response. The viscoelastic response requires complex mathematics (i.e., with real and imaginary terms) to fully describe both the viscous and elastic components. Additionally, the response of soft materials can be highly dependent on the applied strain level; that is, soft materials can have a nonlinear response to applied strain, and so linear viscoelasticity is strictly defined only for infinitesimal small strains. The characterization of the nonlinear

response is traditionally performed on specialized instrumentation.[4] Reducing the complexity of the transformation from the measured instrumental response to the material properties, also called the working equations, is a major design consideration for this type of rheological instrumentation. Rheological measurements, performed in either shear or compression, are confined to one of two well-defined instrumental configurations, which correspond to simplifying limits of the working equations. These two limits are termed *gap loading* or *surface loading*. These instrumental configurations limit the strain level to very small values, typically less than 5%, and produce well-defined flow fields in the sample. These experimental restrictions on the instrumental design are critical for controlling the instrument–sample interactions so that they can be effectively mathematically modeled.

In instrumented indentation, the tip shape and motion produce the instrument–sample interactions and thus define the imposed strains or flow fields, which must be modeled by the components of the working equations. Tip geometries that are currently used, in general, are small versions of classic indenter designs and include flat punches, various rounded probes such as half-spheres, rounded cones, and paraboloidal tips, and pyramidal tips such as the popular Berkovich tip. These designs were originally created to compare the constitutive behavior of metals. For example, because many previously developed hardness test methods were appropriate only for comparing a narrow class of metals, the Vickers hardness test[5] was developed to provide a more continuous scale of hardness with a diamond pyramid indenter. In this case, the Vickers tip geometry was solely based on achieving a desirable ratio of the indentation diameter to the ball diameter in the Brinell hardness test, for which this desirable ratio is with respect to optimizing the test to include a wider range of metals than other hardness tests. The Berkovich pyramid was later suggested as a three-faced analogue to the four-faced Vickers pyramid to provide improved reproducibility in fabrication over the Vickers tip while maintaining the same area function [5]. Similarly, the ease of manufacturability and/or simplification of analysis for elastic–plastic materials led to the use of rounded and flat punch probes.

Analyses of indentation behavior are generally based on elastic contact theories, such as those of Hertz and Sneddon, or extensions for elastic–plastic behavior. For example, nominal indentation stresses and strains have been defined as a function of geometry.[6,7] For a Berkovich pyramidal tip, empirical analyses based on elastic–plastic metals attributed to Tabor[8] yield an estimated characteristic strain of 8–10%, although recent research[3,9] suggests even higher values. The mean stress or hardness, H, is defined as the ratio of the force, P, to the contact area, A, where A is in general related to the displacement, h, by the tip geometry. However, traditional indentation tips produce combinations of shear and compressional deformations of the sample that depend on the particular tip geometry. In contrast to most metals, soft materials are sensitive to the type and level of applied strain. Thus, the use of current indenter tip shapes to characterize soft materials will present difficulties in correlating the measured instrumental response to the actual material properties of the sample. This problem is clearly demonstrated in the following section.

Working Equations for Rheology and Instrumented Indentation

For both classical rheology and instrumented indentation on soft materials, the forces and displacements measured in any mechanical experiment are related to the states of stress and strain by the constitutive equation, which describes the properties sought and the equations of motion and continuity.[4] In classical rheology, the dynamic response of viscoelastic materials is characterized by the use of oscillatory experiments with one of two specific instrumental geometries that correspond to simplifications in the working equations that describe the dynamic instrument–sample interaction. Both specific instrumental geometries limit the applied strain to levels of linear stress response (i.e., deformations are infinitesimal), thus minimizing nonlinear response. The first limit, termed *gap loading*, is defined when the sample dimensions are small with respect to the wavelength of the elastic wave corresponding to the applied steady-state deformation. The inertial forces can be neglected, and the stress–strain ratios are related to force–displacement ratios by simple geometric factors in a gap-loading geometry. A simple example is the use of gap-loading geometry for measurements of the shear storage modulus (G') and loss modulus (G'') of viscoelastic polymer melts. In this case, the sample is con-

fined between two narrowly spaced parallel plates, for which the gap separation is less than or equal to $\lambda_s/50 - \lambda_s$, where λ_s is the shear wavelength. This limit generally sets the upper frequency limit in commercial rheological instrumentation. The propagation of Raleigh shear waves, which have no compressional component, is generated in the sample by the motion of one of the parallel plates and is approximated by a linear shear gradient.[4,10,11] One of the parallel plates is driven with a known harmonic displacement, and the resulting force is measured at the other parallel plate. G' and G'' are given by these extremely simple relationships:

$$G' = \frac{P_0}{bh_0}\cos\delta \tag{1}$$

$$G'' = \frac{P_0}{bh_0}\sin\delta \tag{2}$$

In these equations, P_0 and h_0 are the force and displacement amplitudes, δ is the phase angle between the force and displacement, and b is a geometric factor. These expressions apply only to this extremely specialized instrumental geometry. To demonstrate this point, a simple change can be made so that the force and displacement are measured at the same surface. Now eqs 1 and 2 can no longer be used, and the motion of this surface must be modeled with a more complex expression for the mechanical impedance, Z^*, describing the instrument–sample interaction. A model of a damped harmonic oscillator, which includes a collection of springs and dashpots, such as that shown in Figure 1(a), is typically used, and Z^* is modeled by a parallel arrangement of a spring, S_M, accounting for the sample *elastance* and a dashpot, R_M, accounting for the sample *frictance*, with the terminology of Ferry.[4] This parallel arrangement of spring and dashpot does not correspond to a Voigt/Kelvin constitutive element, as S_M and R_M do not represent the sample modulus and viscosity. Rather, in the case of driving the model in Figure 1(a) by a sinusoidal force, they are related to the real and imaginary components of Z^* as follows:

$$Z^* = R_M + iX_M = R_M + i(\omega M - S_M/\omega - S_M^0/\omega) \tag{3}$$

where ω is the radian frequency, M is the mass of the moving element, $S_M{}^0$ is the elastance of the instrument springs, and R_M and X_M are the mechanical resistance and mechanical reactance.

For this type of experiment, G' and G'' are given by

$$G' = \frac{S_M}{b} \tag{4}$$

$$G'' = \frac{\omega R_M}{b} \tag{5}$$

This subtle shift in instrumental design now requires the direct measurement of the components of the complex mechanical characteristic impedance to characterize the viscoelastic response of the sample. In the gap-loading example, the only requirement was the measurement of the force and displacement amplitudes and the phase angle between them. The mathematics become even more involved if the sample dimensions are not small. For example, when the thickness in the parallel-plate geometry becomes large ($\lambda_s/50 - \lambda_s$,), the inertial forces can no longer be neglected.

The second well-defined instrumental geometry for classical rheology, termed *surface loading*, assumes that the thickness (or other appropriate dimension) is large enough so that the Raleigh shear wave energy propagation generated in the sample by the motion of a transducer in contact with the sample will propagate and dissipate completely with no reflected energy reaching the transducer. The important geometric parameter becomes the contact area, A_s, of the driving surface, and again, the complex mechanical impedance is measured. In the previous example (eqs 4 and 5), S_M and X_M were related only to G', and R_M was related only to G''. In surface loading, however, G' and G'' depend on both R_M and X_M:

$$G' = \frac{(R_M^2 - X_M^2)}{A_s\rho} \tag{6}$$

$$G'' = \frac{2R_M X_M}{A_s\rho} \tag{7}$$

Because inertial forces are now important, the sample density, ρ, is involved in these equations. In this case, knowledge of both components, real and imaginary, of the complex characteristic impedance is required to determine either the storage or loss component of the sample response. All classical shear rheology on soft materials employs one of these two geometries.

Similarly to rheological instrumentation, the dynamic instrument–sample interaction for

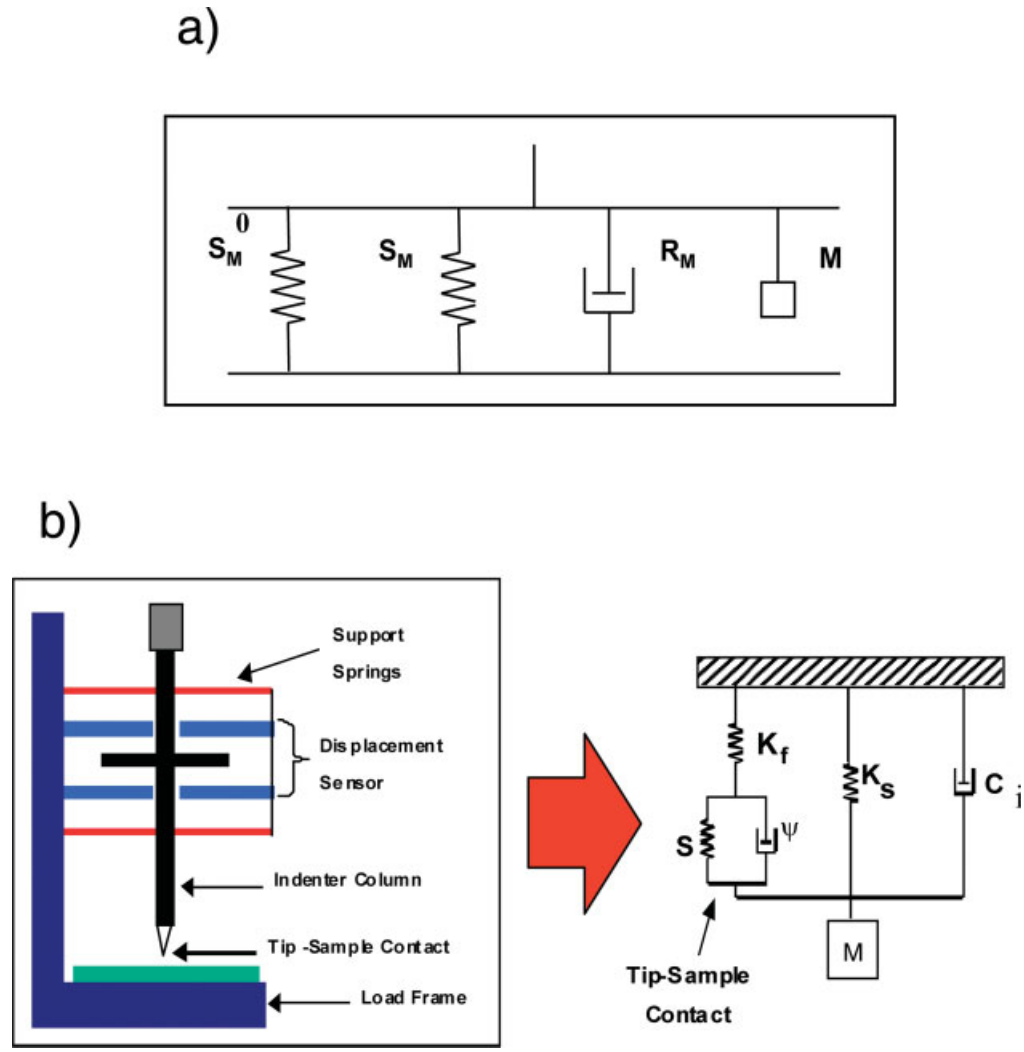

Figure 1. (a) Schematic illustration of the dynamic model of the Birnboim apparatus after Ferry[4] and (b) schematic illustration of a depth-sensing indentation system (left) and a corresponding dynamic model (right) that includes a parallel spring–dashpot element to account for the sample behavior. [Color figure can be viewed in the online issue, which is available at www.interscience.wiley.com]

instrumented indentation of soft materials is based on a damped harmonic oscillator model in which the mechanical impedance of the instrument–sample interaction is again modeled by a parallel arrangement of a spring and a dashpot, as shown in Figure 1(b).[2,12,13] However, unlike rheological instrumentation, the relationships between G' and G'' and R_M and S_M have been assumed with a basis in the elastic solution to the tip–sample contact problem. According to the notation in Figure 1(b), which is common in the instrumented indentation literature, the sample impedance is made up of the tip–sample contact stiffness, S, and the tip–sample damping factor, C_s. Solving for the real and imaginary components of the complex impedance results in expressions for S and C_s:

$$S = \frac{P_0}{h_0}\cos\delta + \omega^2 m - K_{s\rho} \tag{8}$$

$$C_s = \frac{P_0}{h_0}\sin\delta - C_i \tag{9}$$

S is thus a function of calibrated instrument and measured test parameters, including the system spring stiffness K_{sp}, system damping coefficient C_i, system mass m, frequency ω, phase angle δ, magnitude of the force oscillation

P_0, and magnitude of the displacement oscillation h_0. During an indentation measurement with CSM, C_s is assumed to be zero and S is estimated as a function of depth throughout the loading segment with eq 8. The following equation can then be used to calculate the contact depth, h_c, continuously with the measured contact stiffness, displacement h, and load P:

$$h_c = h - \frac{\varepsilon P}{S} \tag{10}$$

In this equation, ε is a geometric constant. Detailed knowledge of the tip shape combined with knowledge of h_c yields an estimate of the contact area, A, continuously, and thus the sample modulus E can be measured continuously with the following equation:[1,14]

$$S = 2aE_r = \frac{2}{\sqrt{\pi}} E_r \sqrt{A} \tag{11}$$

In this equation, the cross section of the indenter is assumed to be circular with respect to the contact radius, a, to the projected area of tip–sample contact, A. A small correction is sometimes applied for noncircular cross sections,[7] and additional minor corrections have also been suggested.[3] The reduced modulus, E_r, accounts for deformation of both the indenter (elastic modulus E_i and Poisson's ratio ν_i) and the sample (elastic modulus E_s and Poisson's ratio ν_s) and is given by

$$\frac{1}{E_r} = \frac{(1-\nu_s^2)}{E_s} + \frac{(1-\nu_i^2)}{E_i} \tag{12}$$

The current calculations of the reduced storage modulus, E_r', and reduced loss modulus, E_r'',[13] are based on the elastic solution for quasi-static indentation, that is, eq 11, which when rearranged yields

$$E_r = \frac{S\sqrt{\pi}}{2\sqrt{A}} \tag{13}$$

Thus, the following equations are used:

$$E_r' = \frac{S\sqrt{\pi}}{2\sqrt{A}} \tag{14}$$

$$E_r'' = \frac{\omega C_s \sqrt{\pi}}{2\sqrt{A}} \tag{15}$$

For an isotropic material, the corresponding values in shear, G_r' and G_r'', are found by the division of E_r' and E_r'', respectively, by $2(1 + \nu)$.

Loubet et al.[15] argued that equations similar to eqs 14 and 15 are based on the principle of elastic–viscoelastic correspondence. In ref. [15], equations for storage and loss moduli are presented in terms of shear, with the $1 - \nu^2$ term missing and ν assumed to be 0.5; this results in a factor of 0.75 between Loubet et al.'s equations and eqs 14 and 15. However, in this case, the correspondence principle has been used incorrectly. First, the correspondence principle applies in the solution of a viscoelastic boundary value problem after a Laplace or other transform is applied to remove time from the system of variables. Such a transformation of variables produces an elastic problem in the transformed variables, the elastic solution of which can be used with the viscoelastic operators in place of the elastic constants; this then yields a solution to the original viscoelastic problem upon transformation back to the time domain. However, for contact mechanics problems, this procedure is not strictly valid, in general, because the boundary conditions change as a function of time. Even if this restriction is ignored mathematically, formulating eqs 14 and 15 by the substitution of the viscoelastic operator, E', for E_r in eq 13 and by the substitutions of E'' for E_r and ωC for S is clearly inappropriate. Rather, the appropriate substitution would be of the viscoelastic operators into, for example, the elastic solutions from Sneddon,[16] which involve the elastic shear modulus. Equation 13 was initially derived from Sneddon's solutions by Pharr et al.,[14] and thus the viscoelastic solution would require replacing the elastic shear modulus with a viscoelastic shear modulus, which is complex in the case of oscillatory deformation, completing the derivation, and transforming back to the time or frequency domain. Complicating this derivation are the potential differences between the quasi-static contact problem and the dynamic contact problem.

A second argument used by Lucas et al.[2] was that of a similarity to dynamic mechanical analysis (DMA), resulting in the following equations:

$$E' = \frac{\sqrt{\pi}}{2\sqrt{A}} \left(\frac{P_0}{h_0} \cos\delta \right) \tag{16}$$

$$E'' = \frac{\sqrt{\pi}}{2\sqrt{A}} \left(\frac{P_0}{h_0} \sin\delta \right) \tag{17}$$

These equations are similar to eqs 1 and 2. However, the assumptions that lead to eqs 1 and 2, namely, gap-loading conditions with the

force and displacement measured at opposite surfaces of parallel plates in simple shear, are certainly not met in the case of instrumented indentation. Rather, the measurement geometry corresponds more closely to that of surface loading, and thus the storage and loss moduli are more likely to be functions of both the real and imaginary parts of the mechanical impedance. Moreover, the storage and loss moduli in eqs 16 and 17 should actually be reduced moduli such that these equations are equivalent to eqs 14 and 15. Thus, eqs 14 and 15 appear to have little physical basis, and the corresponding measurements of the storage and loss moduli are questionable. In this study, dynamic mechanical characterization was performed for a cured epoxy, poly(methyl methacrylate) (PMMA), and poly(dimethyl siloxane) (PDMS) with traditional rheological instrumentation and dynamic indentation, and the results are compared and analyzed.

EXPERIMENTAL

Although the nanoindenter and rheological instrumentation share a common electrostatic or electromagnetic control system ideal for testing soft materials, they approach the problem of characterizing soft materials from opposing perspectives. The nanoindenter was originally designed for hard materials and has been adapted for use in soft materials, whereas rheological instruments were designed for fluid materials and have been adapted for use in soft materials. To facilitate a comparison between the nanoindenter and standard rheological instrumentation, samples must have a modulus that is high enough to be measured with the available nanoindenter, typically greater than 1 MPa. This modulus is too large for rheological devices designed for viscoelastic liquids. Fortunately, deformations in shear and simple extension can be used interchangeably, provided that the deformations are very small.[4] For this reason a rheological solids analyzer was used to measure the dynamic response, and the strain was kept below 0.01. It is expected, therefore, that testing these model materials with both of these devices should yield similar results for the harder, glassy polymer materials and more divergent results for softer, rubbery materials. Four materials were selected, including two glassy polymers (a cured thermoset epoxy resin and commercial PMMA) and two rubbery crosslinked PDMS elastomers.

Materials

The materials used in this study included an amine-cured epoxy, PMMA, and two PDMS samples. Epoxy films approximately 190 μm thick were cast onto silicon wafers in a dry nitrogen atmosphere glovebox with a drawdown technique. Highly pure diglycidyl ether of bisphenol A with a mass per epoxy (DER 332, Dow Chemical) equivalent of 172 g and 1,3-bis(aminomethyl)-cyclohexane were mixed at the stoichiometric ratio. All samples were cured at room temperature for 48 h, and this was followed by postcuring at 130 °C for 2 h. The films were then removed from the silicon substrates with tweezers after immersion in warm water. The glass-transition temperature of the cured films was 123 ± 2 °C, as estimated with DMA. The PMMA sample was obtained from a commercial Plexiglas acrylic sheet from AtoHaas North America, Inc. The PDMS samples were obtained from Dow Corning Corp. The first sample (the stiffer of the two) was a general-purpose (GP-50) silica-filled crosslinked PDMS with a thickness of 3.2 mm. The second PDMS sample was made from Sylgard 184 mixed at a 10:1 (resin/crosslinker) mass ratio. PDMS was cast onto a glass plate and degassed for 30 min under 67.7 kPa of vacuum pressure for 4 h at 65 °C; this resulted in a layer thickness of 2.7 mm.

Solid Rheology Measurements

DMA measurements were measured with a rheological solids analyzer (RSA II, Rheometrics Scientific, Inc.) with the optional environmental control module. This instrument is a displacement-controlled system capable of performing dynamic mechanical tests with controlled displacement amplitude. The amount of strain is determined from the applied displacement and the sample geometry, and a load transducer measures the resulting force. The applied strain for all samples was held below 0.01. Complete frequency scans were performed at a constant temperature starting at 23.0 °C. This frequency scan was repeated at a temperature 5.0 °C lower than that of the previous scan with a final temperature of −50.0 °C. The resulting data were then time–temperature-shifted horizontally to a reference temperature with the Williams–Land-

ell–Ferry approach.[4] Different modes of testing were required for each sample according to the available geometry of the sample and the operating compliance of the instrument. The epoxy and stiffer PDMS sample were tested in tension, whereas PMMA was measured in the three-point bending fixture, and the most compliant PDMS sample was tested in compression.

Nanoindentation Measurements

Nanoindentation was performed with a Nano-Indenter DCM (MTS Systems, Inc.). Dynamic oscillation was superposed over load histories that included an increasing load segment followed by a constant load segment with applied load levels ranging from 5 to 0.01 mN. Harmonic frequencies were varied from 10 to 300 Hz. The displacement amplitude of oscillation was maintained at 5.0 ± 0.5 nm with proportional integral derivative feedback control for the glassy PMMA and epoxy samples. The displacement amplitude was increased to 50 nm for the elastomeric PDMS samples. A Berkovich pyramid probe tip shape was used. The tip shape was measured for these probes with indentation of a fused silica reference sample. Each frequency sweep was performed 10 times, each at a different location on the sample. The reduced storage modulus and reduced loss modulus at each frequency were calculated with eqs 14 and 15, respectively. The storage modulus and loss modulus were subsequently calculated with eq 12 with a Poisson ratio of 0.33 for the glassy polymers and 0.5 for the elastomers. The results displayed for the nanoindentation measurements are the averages of these 10 indentations over a specified range of indentation depths. The characteristic volume of a material measured during indentation experiments typically scales with the cube of the contact radius for axisymmetric indenters. The Berkovich tip makes this approximation difficult because it does not generate a circular contact. However, calculating the contact radius (assuming a circular contact area) from the contact area determined from the indenter area function provides a reasonable approximation. The characteristic volume measured with the glassy systems is approximately 3 μm^3. The required increase in the indentation depths with the elastomer samples increases the characteristic volume to approximately 5500 and 20,000 μm^3 for the two types of PDMS samples.

Dynamic calibrations of the system are typically made with respect to the dynamic model shown in Figure 1.[13] Measuring the dynamic response of the system with no sample is used to obtain the system calibrations. The load-frame stiffness, K_f, is normally assumed to be infinite (i.e., load-frame compliance is zero). By monitoring the amplitude and phase shift, we can use the equations derived for the model to determine the resonance frequency of the system, the system damping coefficient, C_i, the mass, m_i, and the spring constant, K_{sp}. As discussed previously, K_{sp}, which is typically independent of the frequency over a wide frequency range, can be determined from the raw load as a function of the raw displacement, and the system mass can be determined from the displacement at zero load. Also, C_i is often assumed to be independent of the frequency, and this is not necessarily true.

RESULTS AND DISCUSSION

We begin our comparison of the dynamic nanomechanical and bulk properties with polymeric samples within the glassy region of the viscoelastic spectrum. A plot of the dynamic response for cured thermoset epoxy measured with both the solids analyzer and the nanoindenter is shown in Figure 2. The overall good agreement between the data obtained with the solids analyzer and the nanoindenter is apparent. The nanoindentation values are lower than the DMA results by less than a factor of two. The higher frequency values plotted from the solids analyzer experiments were obtained through time–temperature superposition (TTS). This method allows an effective frequency range of over 10 decades for the samples tested here. The values of the shift factor, a_T, used in TTS are shown for all the samples in Figure 3. These factors obey a linear dependence, as expected for TTS. Validation of TTS relationships for nanoindentation data has not been yet demonstrated. Even better agreement between the storage moduli obtained from nanoindentation and the solids analyzer for the glassy PMMA sample is shown in Figure 4. Again, the TTS of the solids analyzer data shows excellent agreement, as expected with the a_T values shown in Figure 3. The loss moduli for the PMMA and the epoxy samples were not plotted because of the large uncertainty in these

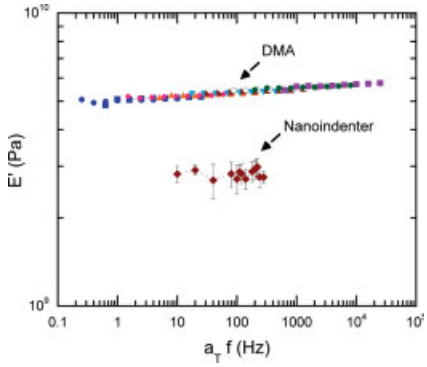

Figure 2. Plot of the frequency (f) dependence of E' for a cured epoxy resin. Both the nanoindentation and dynamic mechanical data are represented, and the dynamic mechanical data have been time–temperature-shifted to a reference temperature of 20 °C. Each symbol represents an average of 10 measurements for the nanoindentation data and a single measurement for the dynamic mechanical data. The error bars represent the corresponding standard deviations ($k = 1$).

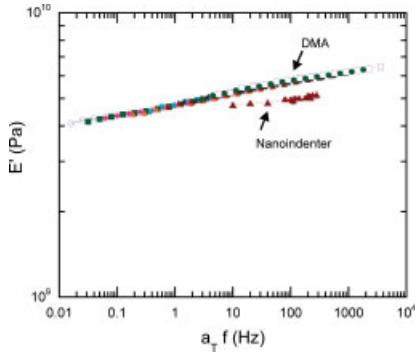

Figure 4. Plot of the frequency dependence (f) of E' for commercial PMMA. Both the nanoindentation and dynamic mechanical data are represented, and the dynamic mechanical data have been time–temperature-shifted to a reference temperature of 20 °C. Each symbol represents an average of 10 measurements for the nanoindentation data and a single measurement for the dynamic mechanical data. The error bars represent the corresponding standard deviations ($k = 1$). The a_T values used for TTS are plotted in Figure 3.

values. The good agreement found for these two glassy samples concurs with the data of Lu et al.[17]

For both the epoxy and the PMMA sample, the nanoindenter appears to capture the frequency dependence (the slope) of the storage modulus. This result is not unexpected because the storage modulus dominates the dynamic response for glassy polymers. However, the larger discrepancy between the indentation data and solids analyzer data for epoxy with respect to PMMA is interesting. Three common sources of uncertainty in nanoindentation experiments with polymers could be considered sources of this disagreement. The first is a proper calibration of the tip area function $A(h_c)$ with the method of Oliver and Pharr.[1] Briefly, a series of indentation measurements are made on a fused silica standard. With a known modulus, the cross-sectional area of the indenter can be measured over a range of contact depths and fit to a multiterm polynomial. The maximum load limit of the DCM apparatus limits indentation depths greater than 750 nm with fused silica. Depths exceeding this limit assume that the area is governed by the lead term of the area function. This term is typically determined from laser reflectance methods[18] and supplied by the manufacturer. The dynamic data reported for the glassy samples were averaged within this valid calibration range (300–800 nm). The characteristic volume of a material tested under these conditions is approximately 3 μm^3. The second source of uncertainty can arise from improper identification of the initial surface contact. An investigation of where the instrument determined surface contact revealed only 10 nm of variability within the 10 indentations. Uncertainty associated with this variability is much less than the standard deviation reported from the 10 measurements. A third consideration may be an inherent strain rate sensitivity difference between the two materials. This could arise from the difference in the microstructures of the thermoset epoxy and thermoplastic PMMA. Creep compliance

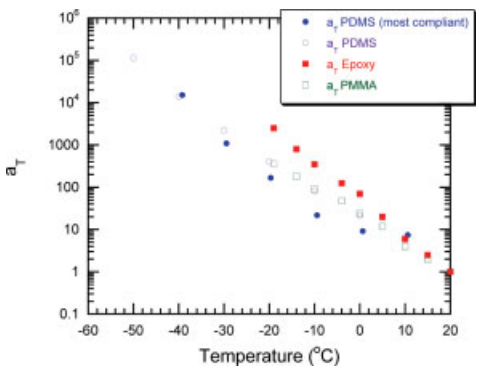

Figure 3. Plot of the a_T values versus the temperature used to time–temperature-shift the data in Figures 2, 4, and 5.

data revealed that the epoxy was more sensitive to an increasing magnitudes of the applied step strain than the PMMA sample. This result may be due to the heterogeneity difference between the two materials. Previous atomic force microscopy using phase contrast imaging of this same epoxy system revealed an angstrom-thick homogeneous layer of material covering heterogeneous domains of hard and soft regions approximately 30 nm in diameter.[19] This length scale is small yet considerably larger than the entanglement length of PMMA.

The PDMS samples, having mechanical behavior that can be described by the rubbery plateau of the viscoelastic spectrum, are considered to be incompressible, ideally elastic, and insensitive to the probe tip shape.[18] The bulk and nanoindenter dynamic data for the stiffer of the two PDMS samples are shown in Figure 5. Although stiff by PDMS standards, this material has a room-temperature modulus that is nearly 3 orders of magnitude lower than the moduli of the glassy materials. As a result, substantially higher displacements are required to resolve force signals. The area function, therefore, is evaluated at displacements outside the fused silica calibration range and depends solely on the lead term of the area function. Despite this uncertainty, good agreement between the bulk and nanoindenter data was observed. A harmonic amplitude of 50 nm was used during the collection of the data. Experiments were also conducted with 5-, 10-, and 25-nm amplitudes, with no significant difference in the measured response. The storage and loss moduli were averaged over indentation depths of 5–10 μm. The characteristic volume of a material tested under these conditions is approximately 5500 μm^3. The time–temperature superimposed solids analyzer data for the storage component show much less scatter than the loss modulus, especially at the lower frequencies. This scatter in the loss modulus is believed to be attributable to the baseline stability in the calibration of the instrument. This result is supported by the observation that the scatter is symmetric about an extrapolated value from higher frequencies. Within each temperature run, the lower frequency data exhibit this scatter. The a_T values, shown in Figure 3, are expected and typical for this material.[4]

The second, more compliant PDMS sample has a modulus that is only half that of the first PDMS. This sample presented significant challenges for identifying the displacement at which the tip first contacted the sample. In Figure 6, the static load is plotted verse the displacement into the surface and illustrates the insensitivity of this signal to surface contact on soft materials. Nearly 2500 nm of displacement was required before 20 μN of force was registered. As mentioned in the introduction, the dynamic contact stiffness (dynamic load signal) can be used to provide much greater sensitivity to surface contact and surface stiffness in comparison with a change in a quasi-static force or stiffness measurement. The inset image illustrates the dynamic contact stiffness signal as the tip approaches the surface, snaps into contact because of surface forces,[20] and measures the increase in the surface stiffness with displacement.

A comparison of the nanoindentation results with those of the bulk rheology obtained for the most compliant PDMS is shown in Figure 7. In this case, the nanoindentation values exceed those measured with the solids analyzer. For additional comparisons, measurements were made on the same PDMS sample in shear with a TA Instruments AR2000 rheometer at a 0.1% strain. (This instrument employs the gap-loading geometry.) Measurements in shear were converted to tension by $2G(1 + \nu)$ under the assumption of $\nu = 0.5$ for PDMS. Spherical probe indentation tests, often called Johnson–

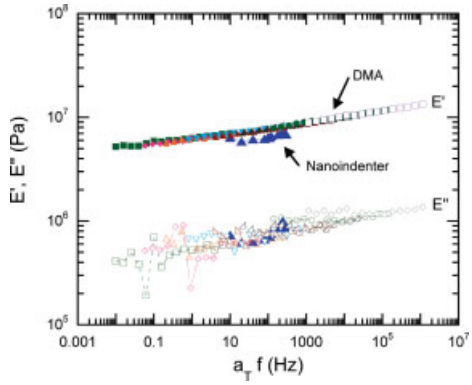

Figure 5. Plot of the frequency (f) dependence of E' and E'' for the stiffer of the two PDMS rubbers. Each symbol represents an average of 10 measurements for the nanoindentation data and a single measurement for the dynamic mechanical data. The error bars represent the corresponding standard deviations ($k = 1$). The dynamic mechanical data have been time–temperature-shifted to a reference temperature of 20 °C. [Color figure can be viewed in the online issue, which is available at www.interscience.wiley.com]

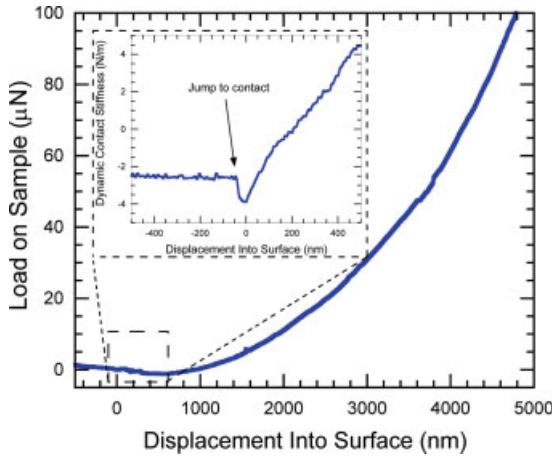

Figure 6. Plot of the static load verse the displacement into the surface for the most compliant PDMS sample. The insensitivity of the load signal to surface contact on soft materials is illustrated by the nearly 2000 nm of displacement before 10 μN of force was measured. The greater surface sensitivity of the dynamic contact stiffness signal is illustrated in the inset image. The dynamic contact stiffness signal snaps into contact as it nears the surface and senses the increase in stiffness with further displacement. [Color figure can be viewed in the online issue, which is available at www.interscience.wiley.com]

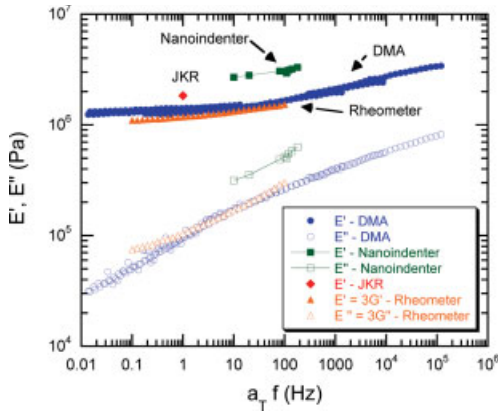

Figure 7. Plot of the frequency (f) dependence of E' and E'' for the most compliant PDMS sample. Each symbol represents an average of 10 measurements for the nanoindentation data and a single measurement for the dynamic mechanical data. The error bars represent the corresponding standard deviations ($k = 1$). The dynamic mechanical data have been time–temperature-shifted to a reference temperature of 23 °C. The nanoindentation results are high with respect to the measured storage and loss components for the dynamic mechanical response measured with the solids analyzer, shear rheometer, and JKR indentation experiments. [Color figure can be viewed in the online issue, which is available at www.interscience.wiley.com]

Kendall–Roberts (JKR) adhesion tests,[21] were also conducted to determine the modulus incorporating adhesion effects. Good agreement was found among all the tests, with the nanoindentation data remaining nearly a factor of 2 higher than those of the other bulk methods. The nanoindenter data were the average storage and loss values reported over indentation depths of 10–15 μm. The characteristic volume of a material tested under these conditions increases to approximately 20,000 μm^3. One plausible reason for elevated values may be the result of underestimating the contact area from inaccurate determination of the lead area function term. The sample stiffness over large displacements can be used to evaluate the compliance of the sample during the indentation experiment and evaluate the uncertainty of the area function. In Figure 8, a plot of the dynamic contact stiffness as a function of the square root of the contact area is shown for the loading portion of the indentation curve obtained with a harmonic frequency of 20 Hz. Through the measurement of the slope of this line with a linear fit, the change in the stiffness over the change in the square root of the contact area can be measured over the majority of the indentation experiment. With the measured slope, a calculation of the storage modulus from the following equation yields a value of

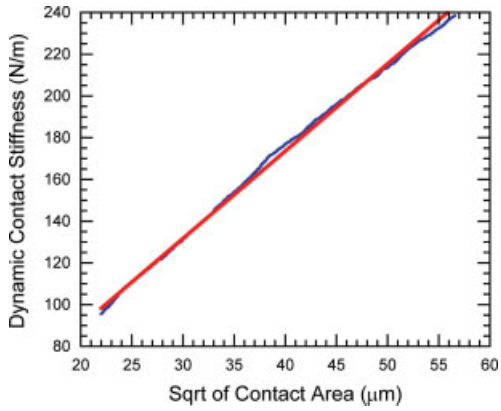

Figure 8. Linear fit of the dynamic contact stiffness over the square root of the contact area obtained from a single indentation experiment. The data correspond to measurements collected over indentation depths of 5–20 μm. The linear dependence suggests a homogeneous material response over these depths and that inaccuracies in the contact area appear not to have played a significant role. [Color figure can be viewed in the online issue, which is available at www.interscience.wiley.com]

2.78 MPa over indentation depths of 5–20 μm:

$$E = \frac{\sqrt{\pi}}{2}\frac{\Delta S}{\Delta\sqrt{A}}(1-\nu_s^2) \qquad (18)$$

This calculation demonstrates that the surface stiffness did not change as a function of the depth. Typically, adjustments of the lead area function term do not result in dramatic changes to the calculated modulus because the modulus depends on the reciprocal of the square root of the area. Thus, inaccuracies in the contact area appear not to have played a significant role.

CONCLUSIONS

The use of instrumented indentation to characterize the dynamic mechanical response of polymeric materials has been compared with the response obtained with more traditional bulk techniques. Four polymer materials were investigated: a cured thermoset epoxy, PMMA, and two PDMS samples. These polymer samples represented materials from the glassy and rubbery plateau regions of the viscoelastic spectrum. The agreement between the dynamic nanoindenter data and the data obtained from a more traditional dynamic mechanical analyzer was good, but it did not match exactly for all the samples. Polymeric materials have the ability to both store and dissipate applied mechanical energy. Although the nanoindenter and classic rheological instrumentation are both based on the damped oscillator theory (with similar dynamic models) and common control systems, the current generation of nanoindenter tip designs produces tip–sample interactions for which there are no analytical solutions. In the absence of an analytical solution, simple analogues to the elasticity-based equation used to calculate the modulus for quasistatic loading are used to generate values of the storage and loss modulus, which themselves have little-to-no physical basis. Regardless of this apparent deficiency, the presented results appear to demonstrate that dynamic mechanical measurements of polymeric materials with nanoindentation surprisingly capture the bulk viscoelastic properties of glassy and elastomeric materials over much smaller length scales than are possible with traditional rheological techniques. The level of agreement found, however, might be because for glassy and elastomeric polymers, energy storage dominates the dynamic response (E' is one to two orders of magnitude larger than E''). Additionally, whether the viscoelastic properties determined with nanoindentation should match exactly measurements from traditional rheological techniques is difficult to assess. Instrument calibration, strain effects, and material heterogeneity are several examples of complications that arise when small volumes of polymers are tested. The slightly more divergent results for epoxy compared with those of PMMA might be indicative of these types of effects. Thus, the current calculation methods, though seemingly adequate for these polymeric materials, will not be able to capture the dynamic response of materials for which viscous or rubbery flow conditions exist (i.e., where energy loss is a more significant factor). These challenges present numerous opportunities for the continued development of indentation instrumentation and techniques.

The authors gratefully acknowledge Matthew Hagon, a contract employee of the U.S. Army Research Lab, for the shear rheology measurements of the poly(dimethyl siloxane), Aaron Forster of the National Institute of Standards and Technology for the Johnson–Kendall–Roberts experiments, Xiaohong Gu of the University of Missouri–Kansas City for sample preparation, and Vincent Jardret and Jenny Hay at MTS Systems Corp. for their help with the test method development. The authors also acknowledge helpful discussions with Don Hunston, Patty McGuiggan, and Sheng Lin-Gibson of the National Institute of Standards and Technology, Greg McKenna of Texas Tech University, and Al Crosby of the University of Massachusetts at Amherst.

REFERENCES AND NOTES

1. Oliver, W. C.; Pharr, G. M. J Mater Res 1992, 7, 1564.
2. Lucas, B. N.; Oliver, W. C.; Swindeman, J. E. In The Dynamics of Frequency Specific Depth-Sensing Indentation Testing, Conference Proceedings Spring MRS Meeting, San Francisco, CA, 1998; Materials Research Society: Warrendale, PA, 1998, Vol. 522, pp 3–14.
3. Dao, M.; Chollacoop, N.; Van Vliet, K. J.; Venkatesh, T. A.; Suresh, S. Acta Mater 2001, 49, 3899–3918.
4. Ferry, J. D. Viscoelastic Properties of Polymers; Wiley: New York, 1980.
5. Dieter, G. E. Mechanical Metallurgy; McGraw-Hill: New York, 1986.
6. Briscoe, B. J.; Fiori, L.; Pelillo, E. J Phys D: Appl Phys 1998, 31, 2395–2405.
7. Shimizu, S.; Yanagimoto, T.; Sakai, M. J Mater Res 1999, 14, 4075.
8. Tabor, D. Hardness of Metals; Clarendon: Oxford, 1951.

9. Chaudhri, M. M. Acta Mater 1998, 46, 3047.
10. Massa, D. J.; Schrag, J. L. J Polym Sci A-2: Polym Phys 1972, 10, 71.
11. White, C. C.; Schrag, J. L. J Chem Phys 1999, 111, 11192.
12. Lucas, B. N.; Oliver, W. C.; Ramamurthy, A. C. Annu Tech Conf Proc 1997, 3, 3445–3449.
13. Asif, S. A. S.; Wahl, K. J.; Colton, R. J. Rev Sci Instrum 1999, 70, 2408–2413.
14. Oliver, W. C.; Pharr, G. M.; Brotzen, F. R. J Mater Res 1992, 7, 613.
15. Loubet, J. L.; Lucas, B. N.; Oliver, W. C. International Workshop on Instrumented Indentation, San Diego, CA, April 22–23, 1995; NIST Special Publication 896; National Institute of Standards and Technology: Gaithersburg, MD, 1995; pp 31–34.
16. Sneddon, I. N. Int J Eng Sci 1965, 3, 47.
17. Lu, H.; Wang, B.; Ma, J.; Huang, G.; Viswanathan, H. Mech Time-Dependent Mater 2003, 7, 189–207.
18. Oliver, W. C.; Pharr, G. M. J Mater Res 2004, 19, 3–20.
19. Gu, X.; Raghavan, D.; Ho, D. L.; Sung, L.; VanLandingham, M. R.; Nguyen, T. Mater Res Soc Symp Proc 2002, Vol. 710, DD10.19.11–DD10.19.16.
20. Pethica, J. B.; Oliver, W. C. Phys Scr T 1987, 19, 61–66.
21. Johnson, K. L.; Kendall, K.; Roberts, A. D. Proc R Soc London Ser A 1971, 324, 301–313.